

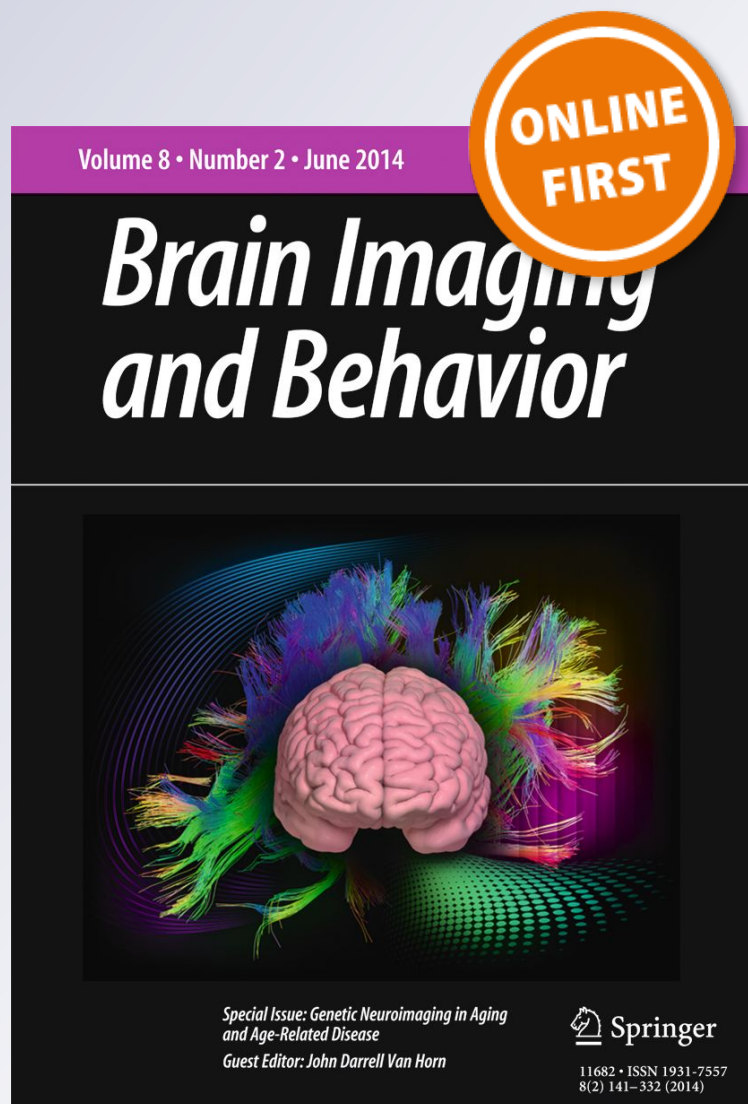
Effective connectivity analysis of inter- and intramodular hubs in phantom sound perception – identifying the core distress network

**Anusha Mohan, Christian Davidson,
Dirk De Ridder & Sven Vanneste**

Brain Imaging and Behavior

ISSN 1931-7557

Brain Imaging and Behavior
DOI 10.1007/s11682-018-9989-7



Your article is protected by copyright and all rights are held exclusively by Springer Science+Business Media, LLC, part of Springer Nature. This e-offprint is for personal use only and shall not be self-archived in electronic repositories. If you wish to self-archive your article, please use the accepted manuscript version for posting on your own website. You may further deposit the accepted manuscript version in any repository, provided it is only made publicly available 12 months after official publication or later and provided acknowledgement is given to the original source of publication and a link is inserted to the published article on Springer's website. The link must be accompanied by the following text: "The final publication is available at link.springer.com".



Effective connectivity analysis of inter- and intramodular hubs in phantom sound perception – identifying the core distress network

Anusha Mohan¹ · Christian Davidson² · Dirk De Ridder³ · Sven Vanneste¹

© Springer Science+Business Media, LLC, part of Springer Nature 2018

Abstract

Tinnitus, the perception of a phantom sound, is accompanied by loudness and distress components. Distress however accompanies not just tinnitus, but several disorders. Several functional connectivity studies show that distress is characterized by disconnectivity of fronto-limbic circuits or hyperconnectivity of default mode/salience networks. The drawback, however, is that it considers only the magnitude of connectivity, not the direction. Thus, the current study aims to identify the core network of the domain-general distress component in tinnitus by comparing whole brain directed functional networks calculated from 5 min of resting state EEG data collected from 310 tinnitus patients and 256 non-tinnitus controls. We observe a reorganization of the overall tinnitus network, reflected by a decrease in strength and efficiency of information transfer between fronto-limbic and medial temporal regions, forming the main hubs of the tinnitus network. Further, a disconnection amongst a subset of these connections was observed to correlate with distress, forming a core distress network. The core distress network showed a decrease in strength of connections specifically going from the left hippocampus/parahippocampus to the subgenual anterior cingulate cortex. Such a disconnection suggests that the parahippocampal contextual memory has little influence on the (paradoxical) value that is attached to the phantom sound and that distress is the consequence of the absence of modulation of the phantom sound.

Keywords Provincial hubs · Connector hubs · Parahippocampus · Disconnection · Tinnitus

Introduction

The disconnection hypothesis was first presented in the schizophrenia literature as a diagnostic construct to explain its pathophysiological mechanisms (Friston and Frith 1995; Weinberger 1993). This hypothesis was that the brain experienced a failure of functional integration of brain areas that may be observed as anatomical disconnections (disruption of white

matter tracts) and/or functional disconnections (disruption of synchronous firing of neurons) (Friston et al. 2016; Friston and Frith 1995). The latter may be measured as the change in functional connectivity between brain areas using different functional imaging techniques such as EEG, fMRI, MEG, etc. However, the term “disconnection” is proposed to represent an aberration in connectivity (anatomical and functional) between brain areas where connectivity may pathologically increase or decrease between different regions (Stephan et al. 2009). With the advent of graph theory, a mathematical tool to conceptualize and empirically calculate different properties of anatomical and functional networks in the brain (Rubinov and Sporns 2010), this disconnection is proposed to manifest as changes in not just connectivity strength but also in the reorganization of brain networks resulting in aberrant functional integration and efficiency of information transfer throughout the network (Bassett et al. 2008; Bullmore and Sporns 2012; Fornito and Bullmore 2015; Stam 2014; Uhlhaas 2013).

This model-based approach to the disconnection hypothesis, may hold not just for schizophrenia, but also for other disorders (Fornito and Bullmore 2014; Fornito et al. 2015).

Electronic supplementary material The online version of this article (<https://doi.org/10.1007/s11682-018-9989-7>) contains supplementary material, which is available to authorized users.

✉ Sven Vanneste
sven.vanneste@utdallas.edu; <http://www.lab-clint.org>

¹ Lab for Clinical & Integrative Neuroscience, School of Behavioral and Brain Sciences, The University of Texas at Dallas, 800 W Campbell Rd, Richardson, TX 75080, USA

² University of Texas Southwestern Medical Center, Dallas, TX, USA

³ Department of Surgical Sciences, Section of Neurosurgery, Dunedin School of Medicine, University of Otago, Dunedin, New Zealand

Tinnitus is the perception of a continuous sound that is theorized to be produced by the brain as a maladaptive compensation to sensory deafferentation, or a failure of noise cancellation (De Ridder et al. 2014b; Mohan and Vanneste 2017). Behaviorally, tinnitus is accompanied by a “non-zero” loudness component and a variable distress component (Elgoyhen et al. 2015; Jastreboff 1990). From a network perspective, tinnitus shows changes in small-world topology characterized by a frequency-dependent increase/decrease in functional connectivity strength and/or reorganization of hubs (Mohan et al. 2016a, b), thereby presenting a functional disconnection between the different regions of the brain network. Furthermore, changes in connectivity strength have been related to changes in tinnitus loudness and distress components, proposing a biomarker for the same (De Ridder et al. 2011b, 2015a; Vanneste et al. 2014).

Tinnitus-related distress is present in about 20% of the tinnitus population (Axelsson and Ringdahl 1989) and manifests as the inability to direct attention to other tasks, rumination on the percept itself, stress, anxiety, decreased cognitive performance, etc. (Görtelmeyer et al. 2011; Vanneste et al. 2016; Zeman et al. 2012). Physiologically, tinnitus-related distress is encoded by a decrease in functional connectivity between fronto-limbic circuits in the alpha frequency band (Chen et al. 2017a, b; Vanneste et al. 2011a, b). It is also encoded by an increase in functional connectivity among regions of the salience network and the limbic system—especially the amygdala, the parahippocampus, and the subgenual anterior cingulate cortex—in the alpha frequency band (Chen et al. 2017a, b; De Ridder et al. 2011c; Vanneste et al. 2014). Thus, functional disconnection (i.e. hypo- or hyperconnection) between specific circuits in tinnitus in the alpha frequency band may be characteristic of the tinnitus-related distress component. The alpha frequency band has been associated with two processes: inhibition and timing. These processes govern two basic qualities of top-down attention: suppression of irrelevant stimuli and selection of salient stimuli (Klimesch 2012; Klimesch et al. 2007). Reduction in alpha power has been attributed to disinhibition in tinnitus and serves as an important neural marker of dysrhythmic thalamocortical oscillations (De Ridder et al. 2015c; Llinás et al. 1999). Furthermore, the distress component of tinnitus is hypothesized to be the behavioral manifestation of hypersalience, or increased top-down attention, which is also encoded in the alpha frequency band (De Ridder et al. 2014a, b). This alpha activity might reflect accelerated theta activity, which is the normal resting state activity of the anterior cingulate cortex (Toth et al. 2007).

Distress is a feature of several disorders and it manifests not just behaviorally but also physiologically. Decreased fronto-limbic connectivity has been shown in other disorders with a strong emotional component, such as bipolar disorder, major

depressive disorder, post-traumatic stress disorder, and schizophrenia (Du et al. 2017; Radaelli et al. 2015; Sripada et al. 2012; Williams et al. 2007). Conversely, increased functional connectivity between the regions of the default mode network and salience network has been shown in schizophrenia (Krishnadas et al.; Zhang et al. 2016). Increased functional connectivity between the regions of the salience network and medial temporal/limbic lobe has been shown in comorbid distress accompanying disorders such as chronic pain, Parkinson's disease, fibromyalgia, dyspnea and social rejection (De Ridder et al. 2011a; Hu et al. 2015; von Leupoldt et al. 2009). Thus, network disconnectivity encoding the emotional component of a disorder seems to be a disorder-general phenomenon that is present in not only tinnitus, but also in other disorders known to have a strong emotional component. Furthermore, the regions involved in the network that encode disorder-general distress seem to be common to multiple pathologies.

Although these studies present evidence for network disconnectivity in several pathologies, they focus on undirected measures that only describe the magnitude of connectivity—i.e. the presence of co-activation—between regions. Effective, i.e. directional, connectivity (Friston 2011) may be calculated using Granger causality, which takes into consideration both the amplitude and phase of the time series and causally infers which region sends information and which one receives it (Pascual-Marqui et al. 2014). However, the studies that employ effective connectivity are usually model-based, hypothesis-driven, or focused on selected regions of interest, as opposed to purely data-driven. In the current study, we calculate effective connectivity using Granger causality and look at the distress network in tinnitus from a data-driven perspective.

The purpose of the current study is to understand the causal organization of a pathological network such as in tinnitus and compare it to a control network. Furthermore, we aim to identify the core network of (disorder-general) distress using a data-driven approach by investigating the hubs in the alpha frequency band based on their involvement within and between functional modules. Based on previous findings, we expect disconnectivity in the pathological network to manifest via changes in connectivity strength and/or hubs of the network. We further hypothesize that the core distress network consists of regions of the fronto-limbic, default mode, and/or salience networks whose connectivity strength shows a significant correlation with distress. Although the neural correlates of distress have been discussed previously, this is the first study that we know of that uses a data-driven approach for empirically identifying the core distress network using effective connectivity. The results of the current study will serve to identify biomarkers for chronic distress, where effective connectivity can point out the causal flow of the

disconnection in the tinnitus network. Since we use a data-driven approach, our results are less subject to biases from a priori assumptions and therefore offer a more objective way of reducing data. Since distress is a disorder-general symptom, the results of the current study may be extended to other pathologies. Further, the results of the current study present an important application in identifying targets for neuromodulation studies that can aim at modifying networks rather than specific regions.

Materials and methods

Tinnitus group

The tinnitus group consisted of 310 participants ($M = 50.63$ years, $Sd = 13.67$ years; 212 males and 98 females), whose percepts' onsets occurred at least a year prior to data collection. Individuals having pulsatile tinnitus, Ménière's disease, otosclerosis, chronic headache, neurological disorders such as brain tumors, or those being treated for mental disorders were excluded from the study. The qualitative aspects of tinnitus that were recorded included location (unilateral ($N = 114$) or bilateral ($N = 197$)) and type (pure-tone ($N = 118$) or noise-like ($N = 193$)). Pure tone audiometric thresholds were collected at .125, .25, .5, 1, 2, 3, 4, 6, and 8 kHz as recommended by the British Society of Audiology. Further diagnostic measurements included identifying the pitch and loudness of the tinnitus in the ear with the strongest sense of the tinnitus percept. This was done by presenting a 1-kHz pure tone at a level 10 dB above the patient's hearing threshold at that frequency in the ear contralateral to that of the tinnitus percept. The pitch of the tinnitus percept was determined by adjusting the frequency of the pure tone until the patient reported that they were matched. The intensity of the pure tone was also changed in order to determine the loudness of the percept. Tinnitus loudness level (in dB SL) ($M = 7.85$ dB SL, $Sd = 8.78$) was then calculated by subtracting the absolute loudness level from the audiometric threshold at the tinnitus frequency ($M = 5143$ Hz, $Sd = 3183$) (Meeus et al. 2011; Meeus et al. 2010). A visual analogue scale (VAS) for loudness ('How loud is your tinnitus?': 0 = 'no tinnitus' and 10 = 'as loud as imaginable') was assessed; the mean VAS for loudness was 5.31 ($Sd = 2.56$). Also, the Tinnitus Questionnaire (TQ) (Meeus et al. 2007) that measures a broad spectrum of tinnitus-related psychological complaints was assessed. The global TQ score can be computed to measure the general level of psychological and psychosomatic distress; the mean score on the TQ was 36.45 ($Sd = 17.32$). Depression and anxiety were evaluated using the Hospital Anxiety and Depression Scale (HADS); the mean score on the depression scale was 6.50 ($Sd = 4.06$) and the mean score on the anxiety scale was 6.52 ($Sd = 3.48$).

Control group

The healthy control group consisted of 256 age-matched participants ($M = 49.78$ years; $Sd = 14.74$; 154 males and 102 females) taken from a database collected at the same center. Individuals with psychiatric and neurological illness, a history of psychiatric disorders and drug/alcohol abuse, records of head injury that resulted in a loss of consciousness, seizures, headaches, or physical disability were excluded from the study. No audiometric testing was done on the individuals in the control group.

Data collection and preprocessing

Data collection

The data were collected under the approval of IRB UZA OGA85. All patients gave an informed consent in accordance with the declaration of Helsinki. The study was approved by the local ethical committee at Antwerp University Hospital. Continuous resting-state electroencephalography (EEG) was recorded for 5 min from participants in all three groups (sampling rate = 500 Hz, band-passed = .15–200 Hz). Subjects were seated upright on a comfortable chair in a fully lit room and were instructed to keep their eyes closed. The EEGs were sampled using Mistar-201 amplifiers (NovaTech <http://www.novatecheeg.com/>) with 19 electrodes arranged in the International 10–20 standard placement (Fp1, Fp2, F7, F3, Fz, F4, F8, T7, C3, Cz, C4, T8, P7, P3, Pz, P4, P8, O1, O2). The electrodes were referenced to digitally linked ears and the impedances were kept under 5 k Ω . Off-line analyses included resampling the data at 128 Hz and filtering using a 2–44 Hz band-pass filter. These data were then exported into Eureka! software (Congedo 2002), where it was plotted and manually inspected for episodic artifacts (including eye blinks, eye movement, teeth clenching, body movement and ECG), which were subsequently removed from the EEG. Average Fourier cross-spectral matrices were then computed for the eight frequency bands previously researched in tinnitus: alpha1 (8–10 Hz) and alpha2 (10–12 Hz).

Data preprocessing

Source reconstruction was generated by estimating the intracerebral electrical sources through standardized low-resolution brain electromagnetic tomography (sLORETA; (Pascual-Marqui 2002)). As a standard practice prior to the execution of the sLORETA algorithm, a common average reference transformation was performed on the data (Pascual-Marqui 2002). sLORETA differs from other source localization algorithms since it does not assume a predefined number of active sources while computing neuronal activity in current density (A/m²). The solution space and the associated

lead field matrix used in the study were those that were implemented using the LORETA-Key software (available at <http://www.uzh.ch/keyinst/loreta.htm>). The neocortical (including the hippocampal and anterior cingulate cortex) MNI-152 volume was divided and labeled according to the sLORETA-Key anatomical template based on probabilities returned by the Deamon Atlas (Lancaster et al. 2000) on a total of 6239 voxels (5 mm³ each).

Granger causality

Granger causality reflects the strength of effective connectivity (i.e. causal interactions) from one region to another by quantifying how much the signal in the seed region can predict the signal in the target region (Geweke 1982; Granger 1969). In other words, it can be considered directed functional connectivity. Granger causality is defined as the log-ratio between the error variance of a reduced model, which predicts one-time series based only on its own past values and that of the full model, which additionally includes the past values of another time series. It is important to note that Granger causality does not imply anatomical connectivity between regions but directional functional connectivity between two sources. sLORETA was used to calculate the effective connectivity between the 84 Brodmann regions in the two alpha frequency bands in the tinnitus and control groups. Each Brodmann area represents one node in the network and the connections between pairs of Brodmann areas represents an edge. The 84 regions of interest are shown in Supplementary Fig. 1 and their names are provided in Table 1. The following graph theoretical parameters were calculated using the Brain Connectivity Toolbox (BCT), which is a Matlab-based toolbox developed by Rubinov and Sporns (Rubinov and Sporns 2010). The different parameters explained below were calculated on the average tinnitus and control networks calculated as the arithmetic mean of the individual connectivity matrices.

Network parameters

Overall connectivity strength – network level and connection level

The connectivity strength between pairs of nodes is indicated by the magnitude of Granger causality between them. The average connectivity strength was calculated as the arithmetic mean of all the connections in the network. This overall connectivity strength was compared between the control and tinnitus groups using repeated-measures ANOVA with group as the between-subject variable and frequency as the repeated measure. Significant differences in individual frequency bands were further investigated using simple contrasts.

The strength of each connection in each of the frequency bands was converted into a Fisher's Z score.

Table 1 List of Brodmann areas used in the study

Brodmann areas	Abbreviation	Name of the Brodmann area
BA01	S1	Primary Somatosensory Cortex
BA02	S2	Secondary Somatosensory Cortex
BA03	S3	Tertiary Somatosensory Cortex
BA04	M1	Primary Motor Cortex
BA05	SPS	Superior Parietal Sulcus
BA06	SMA	Supplementary Motor Area
BA07	SPG	Superior Parietal Gyrus
BA08	Pre-SMA	Pre- Supplementary Motor Area
BA09	DLPFC	Dorsolateral Prefrontal Cortex
BA10	FPC	Fronto-parietal Cortex
BA11	OFC	Orbital Frontal Cortex
BA13	Insula	Insula
BA17	V1	Primary Visual Cortex
BA18	V2	Secondary Visual Cortex
BA19	Cuneus	Cuneus
BA20	ITG	Inferior Temporal Gyrus
BA21	MTG	Medial Temporal Gyrus
BA22	STG	Superior Temporal Gyrus
BA23	PCC1	Posterior Cingulate Cortex1
BA24	dACC	dorsal Anterior Cingulate Cortex
BA25	sgACC	subgenual Anterior Cingulate Cortex
BA27	PHC1	Parahippocampal gyrus1
BA28	HIP1	Hippocampal area1
BA29	RSC1	Retrosplenial Cortex1
BA30	RSC2	Retrosplenial Cortex2
BA31	PCC2	Posterior Cingulate Cortex2
BA32	prACC	pregenual Anterior Cingulate Cortex
BA33	rACC	rostral Anterior Cingulate Cortex
BA34	HIP	Hippocampus
BA35	HIP2	Hippocampal area2
BA36	PHC2	Parahippocampal gyrus2
BA37	OTC	Occipital-Temporal Cortex
BA38	TP	Temporal Pole
BA39	AG	Angular Gyrus
BA40	IPS	IntraParietal Sulcus
BA41	A1	Primary Auditory Cortex
BA42	A2	Secondary Auditory Cortex
BA43	PCG	Postcentral Gyrus
BA44	OPCG	Opercular part of inferior frontal gyrus
BA45	IFG	Inferior Frontal Gyrus
BA46	MPFC	Medial Prefrontal Cortex
BA47	VL PFC	Ventro-Lateral Prefrontal Cortex

Connections with differences in Z scores that resulted in values below -1.96 or above 1.96 were flagged as significant. Further, this comparison between the controls and tinnitus group was corrected for multiple comparison using Bonferroni correction, accounting for the number

of connections in each frequency band. Connections with differences in Z scores that resulted in values below -4.34 or above 4.34 corresponding to a p value of $.0000072$ ($= .05 / (84 * 83)$) were flagged as significant. The other values were considered not significantly different between control and tinnitus groups.

Functional distance and characteristic path length – network level and connection level

Functional integration in the brain is the ability to rapidly combine information from distinct and distant brain areas (Rubinov and Sporns 2010). Measures of functional integration characterize the ease of communication between brain regions, which is commonly based on the concept of a path. In functional networks, paths represent sequences of statistical associations of distinct nodes presenting potential routes of information flow between pairs of brain regions. Path lengths thus estimate the potential for functional integration, with shorter paths characterizing greater functional integration.

The shortest paths between pairs of nodes were calculated from the connectivity strength. As a first step, the effective connectivity matrix was converted to a connection length matrix by taking the reciprocal of the connectivity strength. The shortest path between each pair of nodes was then computed from the connection length matrix using Dijkstra's algorithm (Dijkstra 1959). The characteristic path length is an empirical measure of global connectivity of the directed functional network. This is calculated as the mean of all the shortest paths between every pair of nodes in the network, excluding those whose shortest path length was undefined (i.e. the reciprocal of zero connectivity strength). The characteristic path length was compared between the control and tinnitus groups using repeated-measures ANOVA with group as the between-subject variable and frequency as the repeated measure. Significant differences in individual frequency bands were further investigated using simple contrasts.

The shortest path length between each pair of Brodmann areas in each of the frequency bands was converted into a Fisher's Z score. Connections with differences in Z scores with magnitude below -1.96 or above 1.96 were flagged as significant. Further, this comparison between controls and tinnitus group was corrected for multiple comparison using Bonferroni correction, accounting for the number of connections in each frequency band. Connections with difference in Z scores with magnitude below -4.34 or above 4.34 corresponding to a p value of $.0000072$ ($= .05 / (84 * 83)$) were flagged as significant. The other values were considered not significantly different between control and tinnitus groups.

Clustering coefficient/transitivity

Functional segregation is the ability of the brain to carry out specialized processes in densely interconnected groups of brain regions (Rubinov and Sporns 2010). Measures of functional segregation may be quantified by identifying clusters of nodes within a network. The clustering coefficient is a node-specific measure which identifies the nearest neighbors of each node and determines the degree of local connectivity of the node with its neighbors. This is calculated by estimating the fraction of the number of triangles formed around a node with its two nearest neighbors. The average clustering coefficient is also called the transitivity of a network. Transitivity is calculated as the arithmetic average of the clustering coefficient of each node. The formula to calculate the transitivity of the network is given in (Rubinov and Sporns 2010).

The average clustering coefficient or transitivity was compared between the control and tinnitus groups using repeated-measures ANOVA with group as a between-subject variable and frequency as the repeated measure. Significant differences in individual frequency bands were further investigated using simple contrasts.

Inter-/intramodular connectivity

To determine the inter- and intramodular connectivity of a node in a network, the network is first divided into non-overlapping modules or communities which are groups of nodes defined in a specific way. This is performed using the BCT toolbox in Matlab, wherein the modularity or the ability of the network to be divided into non-overlapping communities is maximized. The number of communities formed also depends on the modularity resolution parameter (γ), which increases the number of modules detected when $\gamma > 1$ and decreases the number of modules detected when $0 < \gamma < 1$. The default modularity resolution parameter is $\gamma = 1$. In the current study, we use $\gamma = 1$ to compute the community structure of the average network in both control and tinnitus groups in the two alpha frequency bands.

Intramodular connectivity (module degree Z score)

Once the network has been divided into modules, the contribution of each node within and between modules may be calculated. The contribution of a node within the module may be determined by a within-module parameter called module degree Z score, which is calculated based on the degree (i.e. number of links) a node has within the module and the total degree of all the nodes in the module. The formula for calculating the module degree Z score is given in (Rubinov and Sporns 2010). This is a measure of intramodular connectivity.

Intermodular connectivity (participation coefficient)

In addition to contributing to information transfer within a module, some nodes also connect different modules together. The intermodular connectivity of a node may be determined by a measure called participation coefficient, which is calculated based on the community structure using the formula given in (Rubinov and Sporns 2010). The participation coefficient is closer to 1 when the link from that node is spread out to more modules and is closer to 0 when all its links are in the same module.

Determining inter-/intramodular hubs and other nodes

The inter- and intramodular hubs otherwise called connector and provincial hubs were determined from the participation coefficient and module degree Z scores calculated for all 84 Brodmann areas in the two alpha frequency bands from the average control and tinnitus networks. These hubs were defined for each frequency band separately. Provincial hubs are described as those which have a high module degree Z score and low participation coefficient (Fornito et al. 2015). Thus, nodes that have a module degree Z score greater than 1 SD above the mean and a participation coefficient less than 1 SD above the mean over all regions were defined as provincial hubs (Mohan et al. 2016a). Connector hubs are described as those nodes that have a high module degree Z score and high participation coefficient (Fornito et al. 2015). Thus, those nodes that have a module degree Z score and a participation coefficient greater than 1 SD above the mean over all the regions were defined as connector hubs (Mohan et al. 2016a).

Other nodes that have a module degree Z score and a participation coefficient less than 1 SD above the mean over all regions were defined as peripheral nodes. The nodes that have a module degree Z score less than 1 SD above the mean but a participation coefficient greater than 1 SD above the mean over all regions were defined as connector nodes. These nodes do not form hubs but may be important for intermodular communication owing to their high participation coefficient.

Determining the core tinnitus distress network

Following the identification of the hubs in the two alpha frequency bands, we compared the connectivity strength between the hubs of the average tinnitus network with the connectivity strength of the same nodes in the average control network in the two alpha frequency bands. If the hubs were common to both groups, then only those hubs that changed in hub property were included. For example, in the alpha1 frequency band, the rostral and subgenual anterior cingulate cortices in the right hemisphere are

identified as provincial hubs in the control group but are identified as connector hubs in the tinnitus group. Thus, these nodes are included as a part of the core network in the alpha1 band in the tinnitus group. However, the left insula is identified as a connector hub in both the groups and hence is not included as a part of the core network. The idea here is that we are only interested in those hubs that are changed in tinnitus vs. controls because these are the hubs that comprise the core tinnitus distress network.

The connectivity strength between the selected nodes in both the groups was converted to a Z score using Fisher's Z transformation. Significant differences in the connectivity strength were determined using a two-tailed threshold of 1.96. Further, this comparison between the controls and tinnitus group was corrected for multiple comparisons accounting for the number of connections in each frequency band. In the alpha1 frequency band, connections with differences in Z scores that resulted in values below -3.03 or above 3.03 corresponding to a p value of $.0012$ ($= .05 / (7*6)$) were flagged as significant. The other values were considered not significantly different between controls and tinnitus. In the alpha2 frequency band, connections with differences in Z scores that resulted in values below -3.54 or above 3.54 corresponding to a p value of $.0002$ ($= .05 / (17*16)$) were flagged as significant. In this exploratory part of the analysis, we consider both the uncorrected and corrected results of the comparison of connectivity strength of the core tinnitus network with corresponding hubs of the control network in order to determine the core tinnitus distress network.

The path length between the distinct hubs of the core distress network was calculated using the same method as mentioned above (Materials and Methods section). The path length between the selected hubs in both the groups was converted to a Z score using Fisher's Z transformation. Significant differences in path length were determined using a two-tailed threshold of 1.96. Further, this comparison between the controls and tinnitus group was corrected for multiple comparisons accounting for the number of connections in each frequency band where in the alpha1 frequency band connections with differences in Z scores that resulted in values below -3.03 or above 3.03 and in the alpha2 frequency band, connections with differences in Z scores that resulted in values below -3.54 and above 3.54 were flagged significant. Other connections were determined not significant.

The connectivity strength of the connections that were identified as significantly different from those in the control group in the two alpha frequency bands using both uncorrected and corrected p values were then partially correlated with TQ score controlling for scores on the VAS for loudness. The significant correlations were corrected for multiple comparisons for the number of connections in each frequency band using the Benjamini-Hochberg False Discovery Rate (FDR) at 25% (Benjamini and Hochberg 1995).

Results

Graph theory parameters

Network-level and connection level differences in connectivity strength

The overall connectivity strength of the tinnitus network was significantly lower than the control network and this effect was significantly moderated by frequency band ($F = 292.42, p < .001$). In the alpha1 ($F = 1808.96, p < .001$) and alpha2 ($F = 1925.58, p < .001$) frequency bands, the overall connectivity strength of the tinnitus network was significantly lower than the controls (Fig. 1a).

At a connection level, we also observe a significant decrease in connectivity strength to and from different nodes. Consistently in both frequency bands, we observe significant reduction in the connectivity strength between regions of the bilateral temporal and medial temporal regions, from the cingulate and specific regions of the frontal cortex to the temporal and medial temporal regions and from the cingulate, temporal and medial temporal regions to specific regions of the frontal cortex. After Bonferroni correction, we observe that this decrease in connectivity strength is primarily present in connections going from the medial, temporal, and parietal regions on the right to the cingulate regions on the left. (Fig. 2a–h).

Characteristic path length

The characteristic path length of the tinnitus network was significantly higher than the control network and this effect was significantly moderated by frequency band ($F = 970.75, p < .001$). In the alpha1 ($F = 2821.48, p < .001$) and alpha2 ($F = 2634.29, p < .001$) frequency band, the characteristic path length of the tinnitus network was significantly higher than the controls (Fig. 1b).

At a connection level, we also observe a significant increase in path length in the connections going to and from the frontal areas to the rest of the cortex, in the connections

to and from the cingulate cortex to the temporal and medial temporal regions in the tinnitus group compared to the control group. After Bonferroni correction, we observe the same pattern in the change in characteristic path length between the controls and tinnitus group. (Supplementary Fig. 2a–h).

Transitivity

The transitivity of the tinnitus network was significantly lower than the control network and this effect was significantly moderated by frequency band ($F = 148.99, p < .001$). In the alpha1 ($F = 262.83, p < .001$) and alpha2 ($F = 258.18, p < .001$) frequency band, the transitivity of the tinnitus network was significantly lower than the controls (Fig. 1c).

Community structure

The tinnitus and control networks are divided into a different number of communities depending on the frequency band. Both networks are divided into 3 communities in the alpha1 frequency band and 2 communities in the alpha2 frequency band. The community structure is shown in Supplementary Fig. 3.

Inter- and intramodular hubs

The provincial hubs, connector hubs, peripheral nodes, and connector nodes in the control and tinnitus networks vary by frequency bands. The different node classifications in the tinnitus and control network in the two alpha frequency bands are shown in Figs. 3a–b and 4a–b. The names of the nodes belonging to each classification in the control and tinnitus network, provided in Supplementary Fig. 4. Figures 3c and 4c, also show the hubs that are distinctly present in the tinnitus network in the alpha1 and alpha2 frequency bands respectively. The tinnitus network is characterized by an absence of peripheral nodes, with the presence of a predominantly left-lateralized network of connector nodes in the auditory cortex extending to the rest of the

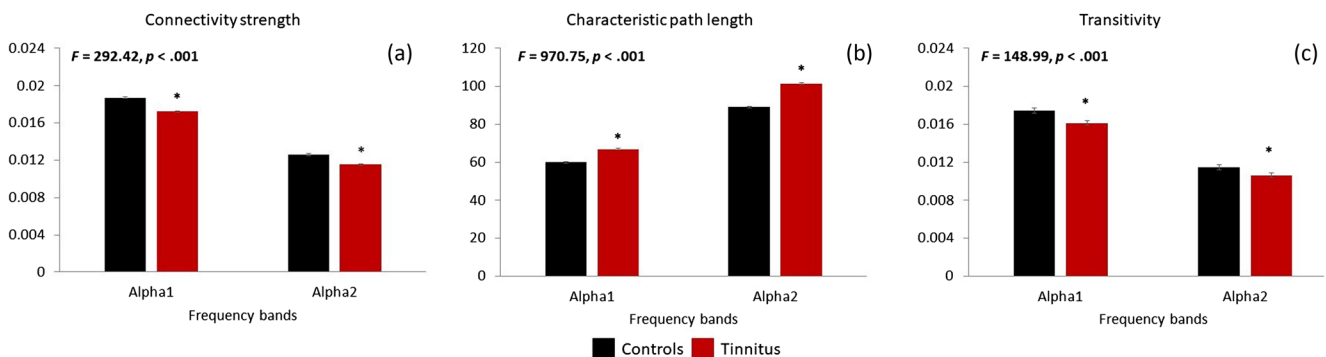


Fig. 1 Graph theoretical parameters calculated from the effective connectivity control (black) and tinnitus (red) networks in the alpha1 and alpha2 frequency bands. **a** Overall connectivity strength, **b** characteristic path length, **c** transitivity in the alpha1 and alpha2 frequency bands

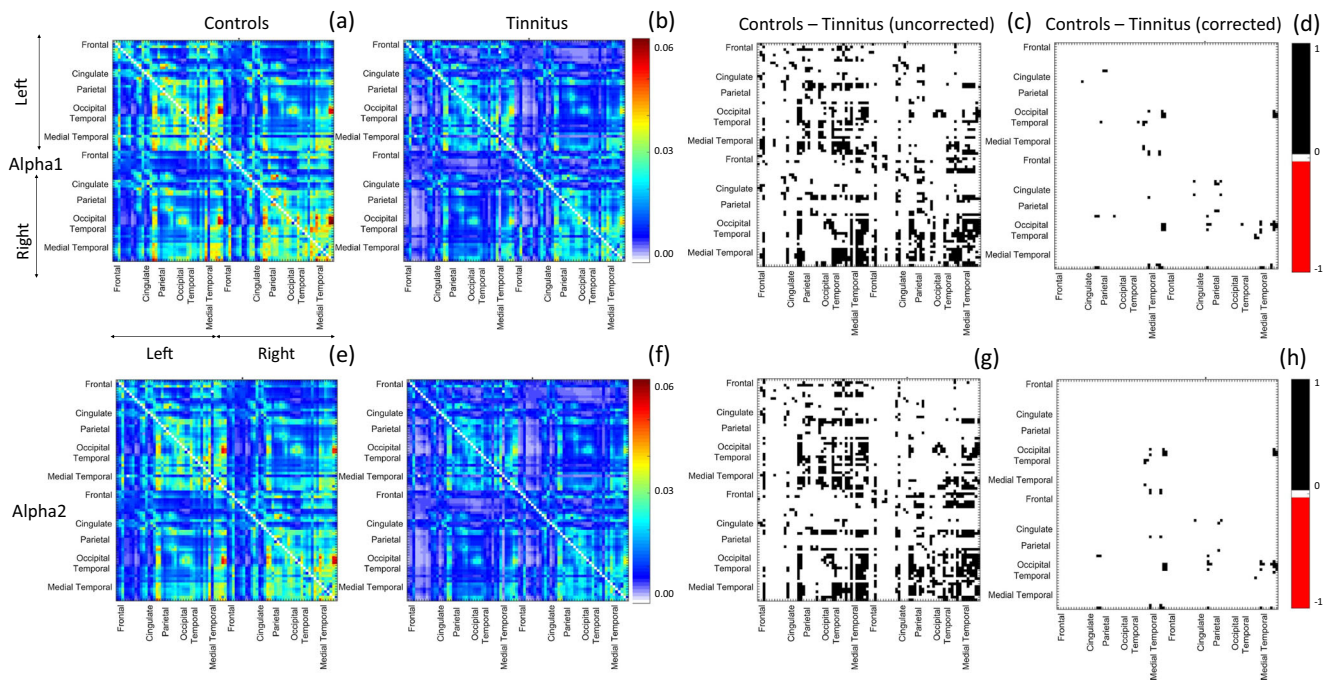


Fig. 2 Comparison of effective connectivity strength between the controls and tinnitus at the connection level. **a, b** Depict the effective connectivity network in the control and tinnitus group respectively and the significant difference in connectivity strength before **(c)** and after **(d)** Bonferroni correction in the alpha1 frequency band. Similarly, **e, f** depict the effective connectivity network in the control and tinnitus group

respectively and the significant difference in connectivity strength before **(g)** and after **(h)** Bonferroni correction in the alpha2 frequency band. Connections with significantly greater connectivity strength in controls are shown in black, connections with significantly greater connectivity strength in tinnitus are shown in red and connections with no significant difference in connectivity strength are shown in white

anterior temporal lobe, as well as the motor cortex and anterior cingulate cortex. Provincial hubs are present in the right posterior cingulate cortex and connector hubs in the right rostral and subgenual anterior cingulate cortex, and left insula and subgenual anterior cingulate cortex. In other words, the connector hubs are located in a bilateral salience network. The names of these hubs are given in Table 2.

Comparing the connectivity strength and characteristic path length between the core tinnitus and control networks

On comparing the connectivity strength between the distinct hubs of the tinnitus network with the same connections in the controls we observe that, in the alpha1 frequency band, there is decreased connectivity strength from the inferior temporal gyrus, posterior and subgenual anterior cingulate to most of the other regions. After Bonferroni correction, we observe that the connectivity strength of the connections from the left inferior temporal gyrus to most of the other hubs and from the right posterior cingulate cortex to the left inferior temporal gyrus and left auditory cortex were decreased (Fig. 3d–g). In the alpha2 frequency band, we observe decreased connectivity

strength from the left insula, inferior, temporal and superior temporal gyrus, dorsal and subgenual anterior cingulate cortex, hippocampus, parahippocampus, right inferior frontal gyrus and ventrolateral prefrontal cortex to most of the other hubs. After Bonferroni correction, we observe that most of these differences still hold (Fig. 4d–g).

On comparing the path length between the distinct hubs of the tinnitus network with the same connections in the controls, we observe a significant increase in path length in the tinnitus group compared to the control group. In the alpha1 frequency band, we observe a significant increase in path length from most of the hubs to the left superior temporal gyrus, left secondary auditory cortex, and right rostral anterior cingulate cortex. We also observe a significant increase in the path length from the right posterior cingulate cortex to the rest of the hubs and the right rostral anterior cingulate cortex to most of the other hubs. In the alpha2 frequency band, we observe significant changes in path length focused in the connections going from and to the right temporal pole, inferior frontal gyrus and to the left subgenual anterior cingulate cortex. After Bonferroni correction, we observe that most of these differences still hold (Supplementary Fig. 5).

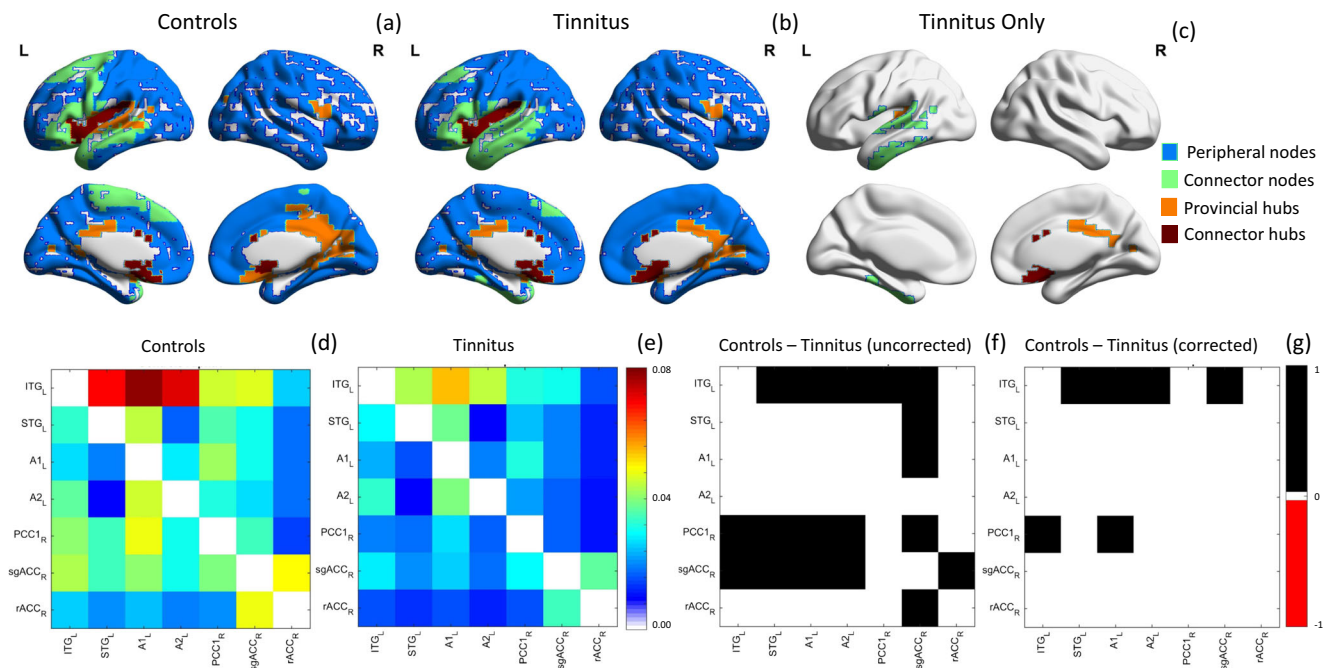


Fig. 3 Display of hubs and comparison of effective connectivity between hubs in the alpha frequency band. **a–c** Display the peripheral nodes, connector nodes, provincial hubs and connector hubs in the **a** average control network; **b** average tinnitus network and **c** the distinct hubs of the tinnitus network. **d–g** Depict the effective connectivity in the **d** control group; **e** tinnitus group; **f, g** the significant difference in connectivity

strength between controls and tinnitus before and after Bonferroni correction respectively. Connections with significantly greater connectivity strength in controls are shown in black, connections with significantly greater connectivity strength in tinnitus are shown in red and connections with no significant difference in connectivity strength are shown in white

Partial correlation of connectivity strength of specific connections with TQ score controlling for VAS for loudness

We observe a significant negative correlation of the connectivity strength between some connections between the hubs of the tinnitus network that have significantly different connectivity strength than the control network that were determined based on the uncorrected *p* value. This includes the connection from the right rostral anterior cingulate cortex to the right subgenual anterior cingulate cortex in the alpha1 frequency band ($r = -.17, p = .003$) and the connections from right ventrolateral prefrontal cortex to the right inferior frontal gyrus ($r = -.18, p = .003$), left hippocampus to left subgenual anterior cingulate cortex ($r = -.18, p = .003$), right inferior frontal gyrus to right temporal pole ($r = -.17, p = .005$), right inferior frontal gyrus to right ventrolateral prefrontal cortex ($r = -.16, p = .007$), left primary somatosensory cortex to left superior temporal gyrus ($r = -.16, p = .007$), left somatosensory cortex to left insula ($r = -.16, p = .008$), left hippocampus to right subgenual anterior cingulate cortex ($r = -.16, p = .008$), left parahippocampus to left subgenual anterior cingulate cortex ($r = -.16, p = .009$), left primary somatosensory cortex to left secondary

auditory cortex ($r = -.16, p = .009$), left subgenual anterior cingulate cortex to right ventrolateral prefrontal cortex ($r = -.15, p = .013$), left parahippocampus to left hippocampus ($r = -.14, p = .013$) and right subgenual anterior cingulate cortex to right temporal pole ($r = -.14, p = .02$) in the alpha2 frequency band (Fig. 5). On correlating the connectivity strength of the connections with significant difference in connectivity strength in the tinnitus group after Bonferroni correction, with TQ score, we observed a significant negative correlation between the connectivity strength of the connections from the left hippocampus to the left subgenual anterior cingulate cortex ($r = -.18, p = .003$), the right inferior frontal gyrus to the right temporal pole ($r = -.17, p = .005$) and from the left hippocampus to the right subgenual anterior cingulate cortex ($r = -.16, p = .008$) (Fig. 6a–c). No significant correlations were observed between all other connections. The correlation coefficient for all the significant connections before Bonferroni correction in the alpha1 and alpha2 frequency bands is provided in Tables 3 and 4. The correlation coefficient for all the significant connections after Bonferroni correction in the alpha1 and alpha2 frequency bands is provided in Tables 5 and 6. The schematic of the core tinnitus distress network is shown in Fig. 7.

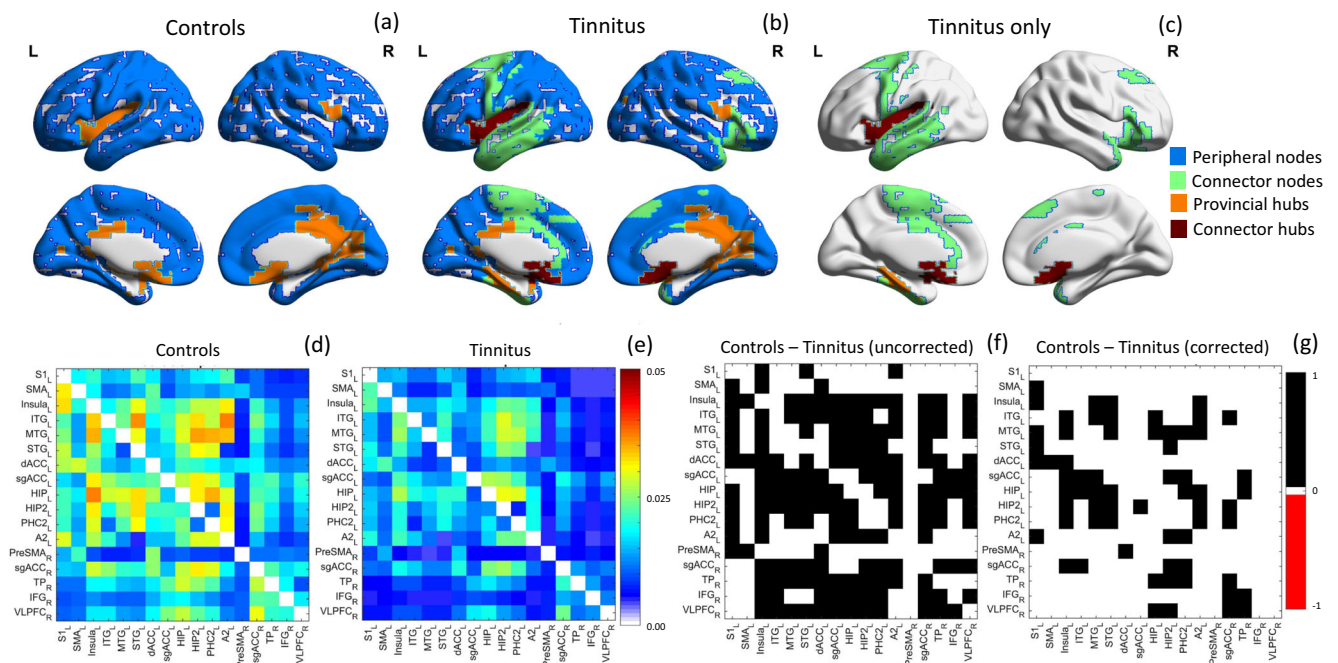


Fig. 4 Display of hubs and comparison of effective connectivity between hubs in the alpha2 frequency band. **a–c** display the peripheral nodes, connector nodes, provincial hubs and connector hubs in the **a** average control network; **b** average tinnitus network and **c** the distinct hubs of the tinnitus network. **d–g** depict the effective connectivity in the **d** control group; **e** tinnitus group; **f**, **g** the significant difference in connectivity

strength between controls and tinnitus before and after Bonferroni correction respectively. Connections with significantly greater connectivity strength in controls are shown in black, connections with significantly greater connectivity strength in tinnitus are shown in red and connections with no significant difference in connectivity strength are shown in white

Discussion

This study systematically examined the effective connectivity describing a disorder-general distress network by evaluating distress in tinnitus patients. First, some graph theory parameters were calculated from the effective connectivity in the whole brain of tinnitus patients in comparison to non-tinnitus healthy controls. Subsequently, the effective connectivity strength between controls and tinnitus patients is calculated at the connection level. Then, zooming in further, the connector nodes, provincial hubs and connector hubs specifically for tinnitus are computed, followed by the comparison of effective connectivity strength between these distinct hubs of tinnitus network with corresponding connections in the control network. To delineate which of these nodes and hubs form parts of the distress network, partial correlation of effective connectivity strength is calculated between specific

connections of the core tinnitus network with TQ score controlling for VAS loudness.

At the network-level, we observe a decrease in overall connectivity strength, clustering coefficient and increase in characteristic pathlength in the tinnitus network in both alpha frequency bands. These results agree with a previous study (Mohan et al. 2016b), suggesting a decrease in functional segregation and integration, or in other words, a disconnection between the nodes within a module and nodes connecting different modules, respectively (Ed Bullmore and Sporns 2009; Rubinov and Sporns 2010). As a result, the network possibly shifts from the normal small-world topology that balances efficiency of information transfer through the network with the metabolic cost of wiring the network (Bullmore and Sporns 2012; Sporns 2013; Watts and Strogatz 1998) to a more lattice topology characterized by decreased efficiency of long-distance communication

Table 2 Names of the hubs present exclusively in the tinnitus network

Frequency band	Areas
Alpha1	Left: ITG, STG, A1, Right: PCC1, sgACC, rACC
Alpha2	Left: S1, SMA, Insula, ITG, STG, dACC, sgACC, HIP, HIP2, A2 Right: PreSMA, sgACC, TP, IFG, VLPFC

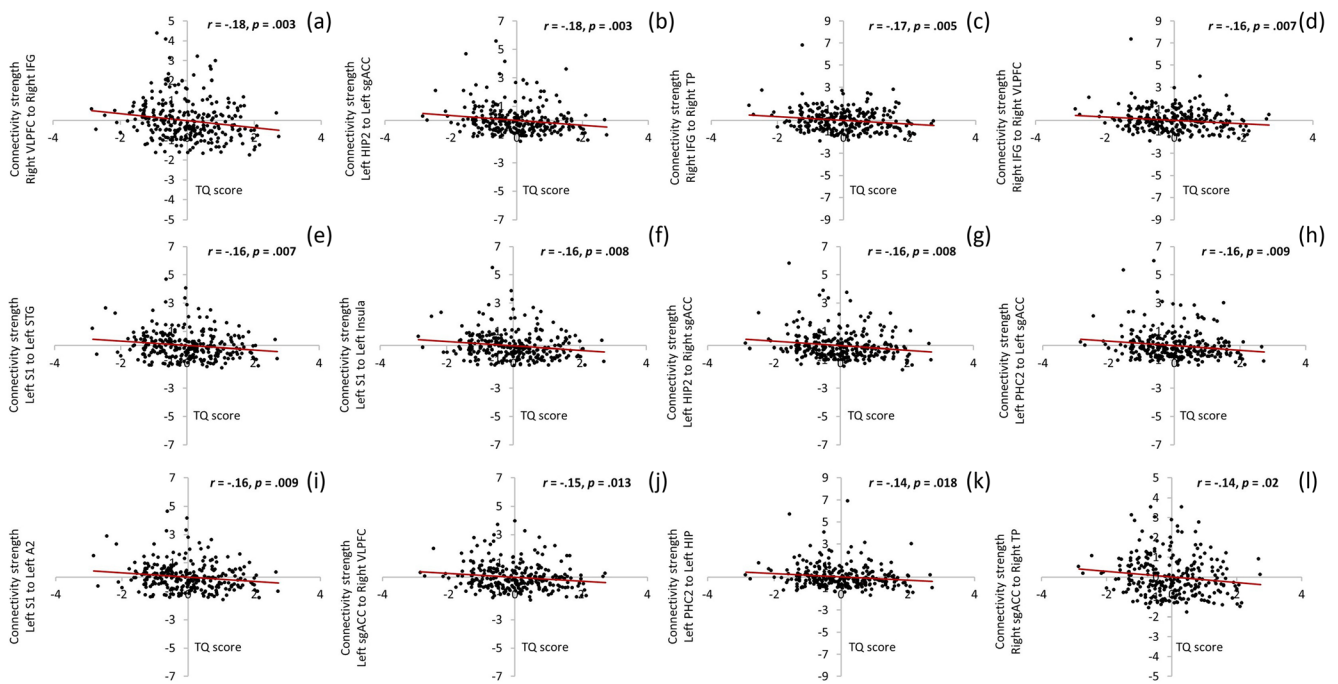


Fig. 5 Partial correlation of effective connectivity strength between specific connections of the core tinnitus network with TQ score controlling for VAS for loudness. These connections are a subset of the connections with a significant change in their connectivity strength before

Bonferroni correction. The values represented in **a–l** are the standardized residuals obtained by independently regressing the connectivity strength and TQ score with VAS for loudness

(Bullmore and Sporns 2012; Sanz-Arigita et al. 2010; Watts 1999; Watts and Strogatz 1998). Such a disconnection and network reorganization may be confirmed by comparing the inter- and intramodular hubs in the two groups and the changes in connectivity strength and pathlength of the connections amongst the hubs of the tinnitus network and those between the hubs and the rest of the cortex.

The hubs play a crucial role in any network because they interact with each other forming a core network that acts as the central control for information transfer within and between modules (Bullmore and Sporns 2012). In the tinnitus network, we first observe a reorganization of the provincial and

connector hubs in both the alpha frequency bands, confirming our previous findings (Mohan et al. 2016a). The hubs distinctly present in the tinnitus network contain regions from the frontal, temporal, medial temporal and cingulate cortices which interact with one another to form the core tinnitus network. Further, we observe a decrease in connectivity strength and increase in pathlength of the connections within the core tinnitus network as well as of the connections going to and from the frontal, cingulate, temporal and medial temporal regions to the rest of the cortex. These variations confirm the disconnection within and between modules in the tinnitus network and that they are mainly controlled by changes in

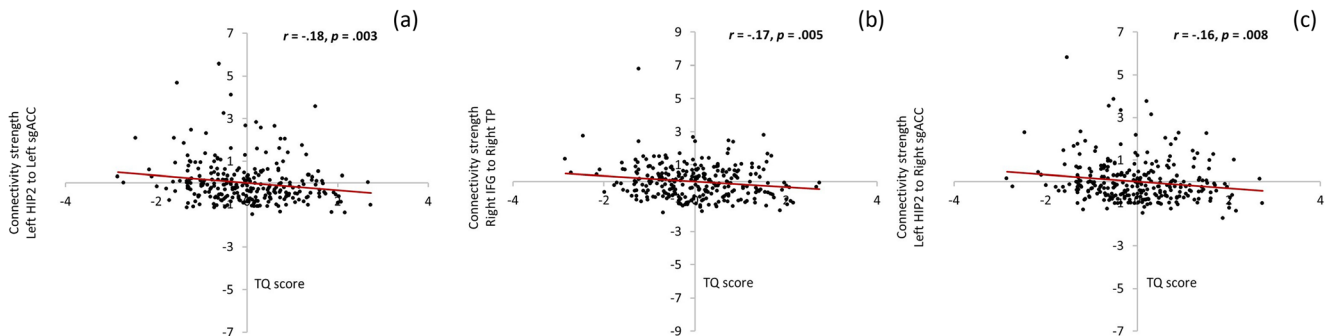


Fig. 6 Partial correlation of effective connectivity strength between specific connections of the core tinnitus network with TQ score controlling for VAS for loudness. These connections are a subset of the connections with a significant change in their connectivity strength after

Bonferroni correction. The values represented in **a–c** are the standardized residuals obtained by independently regressing the connectivity strength and TQ score with VAS for loudness

Table 3 Correlation of connectivity strength of connections between hubs of tinnitus network that showed a significant difference in connectivity strength before Bonferroni correction in alpha1 frequency band and TQ score controlling for VAS for loudness

Connections	r	p value
Right rACC to Right sgACC	-0.18	0.003
Right sgACC to Right rACC	-0.10	0.102
Right PCC1 to Left STG	-0.08	0.175
Left A1 to Right sgACC	-0.08	0.181
Right PCC1 to Left A2	-0.08	0.186
Left ITG to Right ACC	-0.08	0.201
Left STG to Right sgACC	-0.07	0.227
Right PCC1 to Left A1	-0.07	0.253
Right PCC1 to Right sgACC	-0.06	0.288
Right PCC1 to Left ITG	-0.06	0.308
Left ITG to Left A1	-0.04	0.523
Left ITG to Left A2	-0.04	0.550
Left ITG to Left STG	-0.03	0.584
Right sgACC to Left ITG	0.03	0.664
Right sgACC to Left A2	-0.02	0.725
Right sgACC to Left STG	-0.02	0.735
Left ITG to Right PCC1	-0.02	0.756
Right sgACC to Left A1	-0.01	0.853

Significant correlations in bold after correction for multiple comparisons using Benjamini Hoshburg False Discovery rate of 25%

communication between inter- and intramodular hubs (Mohan et al. 2016a). The disconnection of a pathological network mainly affecting its hubs has been reported in several disorders such as schizophrenia, Alzheimer's disease, dementia, Parkinson's disease etc., where the network shifts to a less efficiently wired topology as compared to a control network (Bassett et al. 2008; Crossley et al. 2014; de Haan et al. 2009; Olde Dubbelink et al. 2014; Krishnadas 2014).

The connectivity strength of a subset of these core network disconnections negatively correlate with tinnitus distress, showing that as the disconnection between the hubs increases, the distress increases. We propose this subset of regions, whose connections correlate with distress to form the core distress network which consists of the left parahippocampus and left hippocampus, subgenual anterior cingulate cortex, right ventrolateral prefrontal cortex, right inferior frontal gyrus and right temporal pole. Furthermore, the left parahippocampus and hippocampus send less information to the subgenual anterior cingulate cortex, which in turn sends less information to the right ventrolateral prefrontal cortex, which relays less information to the right inferior frontal gyrus and from there less information is relayed to the right temporal pole.

The left parahippocampus and hippocampus are involved in auditory memory and tinnitus perception (De Ridder et al.

Table 4 Correlation of connectivity strength of connections between hubs of tinnitus network that showed a significant difference in connectivity strength before Bonferroni correction in alpha2 frequency band and TQ score controlling for VAS for loudness

Connections	r	p value
Left HIP2 to Left HIP	-0.18	0.002
Right VLPFC to Right IFG	-0.18	0.003
Left HIP2 to Left sgACC	-0.18	0.003
Right IFG to Right TP	-0.17	0.005
Right IFG to Right VLPFC	-0.16	0.007
Left S1 to Left STG	-0.16	0.007
Left S1 to Left Insula	-0.16	0.008
Left HIP2 to Right sgACC	-0.16	0.008
Left PHC2 to Left sgACC	-0.16	0.009
Left S1 to Left A2	-0.16	0.009
Left sgACC to Right VLPFC	-0.15	0.013
Left PHC2 to Left HIP	-0.14	0.018
Right sgACC to Right TP	-0.14	0.020
Right sgACC to Right IFG	-0.14	0.024
Left PHC2 to Right sgACC	-0.14	0.024
Left HIP to Right VLPFC	-0.13	0.027
Right sgACC to Right VLPFC	-0.13	0.027
Left dACC to Right sgACC	-0.13	0.029
Left HIP2 to Right TP	-0.13	0.033
Left dACC to Left HIP	-0.13	0.036
Left Insula to Left sgACC	-0.13	0.037
Left HIP2 to Right VLPFC	-0.12	0.038
Left sgACC to Right TP	-0.12	0.041
Left HIP to Right TP	-0.12	0.042
Left dACC to Left sgACC	-0.12	0.050
Left ITG to Left sgACC	-0.12	0.050
Left Insula to Right sgACC	-0.11	0.059
Left dACC to Right VLPFC	-0.11	0.067
Left Insula to Left HIP	-0.11	0.068
Left PHC2 to Right TP	-0.11	0.077
Left dACC to Right TP	-0.11	0.078
Left HIP2 to Left ITG	-0.10	0.082
Left HIP2 to Left MTG	-0.10	0.085
Left dACC to Left Insula	-0.10	0.085
Left ITG to Right VLPFC	-0.07	0.244
Left HIP to Left Insula	-0.07	0.253
Left Insula to Left PHC2	-0.07	0.264
Left HIP2 to Left dACC	-0.07	0.265
Left HIP2 to Left A2	-0.07	0.269
Left HIP2 to Left STG	-0.07	0.282
Left ITG to Right TP	-0.06	0.287
Left SMA to Left dACC	-0.06	0.288
Left MTG to Left HIP	-0.06	0.294
Left A2 to Left Insula	-0.06	0.298
Left dACC to Left PHC2	-0.06	0.304
Left Insula to Right TP	-0.06	0.313

Table 4 (continued)

Connections	r	p value
Left HIP to Left A2	-0.06	0.327
Left MTG to Right VLPFC	-0.06	0.333
Left sgACC to Left dACC	-0.06	0.334
Left STG to Left Insula	-0.06	0.336
Left HIP to Left dACC	-0.06	0.347
Left STG to Left PHC2	-0.06	0.351
Left dACC to Left SMA	-0.06	0.363
Left HIP to Left MTG	-0.05	0.365
Left MTG to Right TP	-0.05	0.366
Left ITG to Left MTG	-0.05	0.369
Left HIP to Left STG	-0.05	0.374
Left STG to Left HIP2	-0.05	0.377
Right PreSMA to Left dACC	0.05	0.379
Right sgACC to Left Insula	-0.05	0.381
Left Insula to Left dACC	-0.05	0.391
Left A2 to Left S1	-0.05	0.396
Left PHC2 to Left A2	-0.05	0.419
Left STG to Left S1	-0.05	0.419
Right PreSMA to Left S1	0.05	0.437
Right PreSMA to Left SMA	0.05	0.455
Left PHC2 to Left STG	-0.04	0.462
Right TP to Left sgACC	-0.04	0.464
Left Insula to Left SMA	-0.04	0.465
Left ITG to Left A2	-0.04	0.467
Left sgACC to Left A2	-0.04	0.469
Left MTG to Left S1	-0.04	0.481
Left sgACC to Left STG	-0.04	0.486
Left ITG to Left Insula	-0.04	0.491
Left MTG to Left Insula	-0.04	0.491
Right sgACC to Left dACC	-0.04	0.493
Right IFG to Left sgACC	-0.04	0.494
Right VLPFC_Left STG	0.00	0.952
Right IFG_Left HIP	0.00	0.972
Right TP_Left dACC	0.00	0.979
Right TP_Left HIP	0.00	0.985
Right VLPFC_Left Insula	0.00	0.988
Left ITG_Left HIP2	0.01	0.909
Right VLPFC_Left MTG	-0.01	0.917
Left MTG_Left A2	0.01	0.919
Left PHC2 to Right VLPFC	-0.10	0.088
Left A2 to Left sgACC	-0.10	0.099
Left STG to Left sgACC	-0.10	0.099
Left Insula to Left MTG	-0.10	0.099
Left HIP2 to Left Insula	-0.10	0.104
Left A2 to Left HIP	-0.10	0.105
Left PHC2 to Left MTG	-0.10	0.107
Right VLPFC to Left sgACC	-0.10	0.115
Left SMA to Left Insula	-0.09	0.117
Left PHC2 to Left Insula	-0.09	0.118

Table 4 (continued)

Connections	r	p value
Left HIP to Right sgACC	-0.09	0.127
Left STG to Left HIP	-0.09	0.128
Left A2 to Right sgACC	-0.09	0.130
Left STG to Right sgACC	-0.09	0.131
Left HIP to Left sgACC	-0.09	0.132
Left HIP to Right IFG	-0.09	0.134
Right VLPFC to Right sgACC	-0.09	0.141
Left ITG to Right sgACC	-0.09	0.151
Left MTG to Left sgACC	-0.09	0.151
Left sgACC to Left Insula	-0.09	0.153
Left SMA to Left S1	-0.09	0.158
Right VLPFC to Right TP	-0.08	0.173
Right IFG to Right sgACC	-0.08	0.174
Left sgACC to Right IFG	-0.08	0.178
Left Insula to Right VLPFC	-0.08	0.182
Left A2 to Left PHC2	-0.08	0.188
Left dACC to Left STG	-0.08	0.195
Left dACC to Left ITG	-0.08	0.195
Left dACC to Left A2	-0.08	0.204
Left MTG to Right sgACC	-0.08	0.212
Left A2 to Left HIP2	-0.07	0.224
Left dACC to Left HIP2	-0.07	0.227
Left ITG to Left HIP	-0.07	0.232
Right TP to Right sgACC	-0.07	0.240
Left Insula to Left STG	-0.04	0.502
Left HIP to ITG	-0.04	0.510
Left Insula to Left A2	-0.04	0.512
Left Insula to Left HIP2	-0.04	0.525
Right TP to Left HIP2	0.03	0.565
Left sgACC to Left MTG	-0.03	0.568
Left MTG to Left PHC2	-0.03	0.577
Right TP to Left ITG	0.03	0.586
Right VLPFC to Left HIP	-0.03	0.594
Left sgACC to Left HIP2	-0.03	0.605
Left ITG to Left STG	-0.03	0.605
Left HIP to Left PHC2	-0.03	0.620
Right TP to Left PHC2	0.03	0.629
Left PHC2 to Left S1	-0.03	0.635
Left MTG to Left HIP2	-0.03	0.638
Right sgACC to Left MTG	-0.03	0.646
Right sgACC to Left STG	-0.03	0.658
Right sgACC to Left A2	-0.03	0.664
Left dACC to Left S1	-0.02	0.687
Right VLPFC to Left dACC	-0.02	0.694
Right IFG to Left HIP2	0.02	0.697
Left sgACC to Left ITG	-0.02	0.699
Left ITG to Left dACC	-0.02	0.699
Left HIP2 to Left S1	-0.02	0.701
Left Insula to Left S1	-0.02	0.702

Table 4 (continued)

Connections	r	p value
Left sgACC to Left PHC2	-0.02	0.719
Right TP to Left Insula	0.02	0.727
Right IFG to Left ITG	0.02	0.770
Right sgACC to Left HIP2	-0.02	0.771
Left ITG to Left S1	-0.02	0.775
Left HIP to Left S1	-0.02	0.781
Right VLPFC to Left ITG	0.02	0.794
Right IFG to Left PHC2	0.02	0.794
Right VLPFC to Left HIP2	0.02	0.794
Right VLPFC to Left PHC2	0.02	0.800
Right TP to Left MTG	0.01	0.807
Left MTG to Left STG	0.01	0.813
Right TP to Left STG	0.01	0.817
Right IFG to Left dACC	0.01	0.831
Right IFG to Left Insula	0.01	0.838
Right sgACC to Left PHC2	-0.01	0.855
Right sgACC to Left ITG	-0.01	0.892
Right TP to Left A2	0.01	0.894

Significant correlations in bold after correction for multiple comparisons using Benjamini Hoshburg False Discovery rate of 25%

2006, 2011a; De Ridder and Vanneste 2014; Laureano et al. 2014; Song et al. 2012), and more specifically in auditory contextual memory (Aminoff et al. 2007, 2013). This suggests that distress in tinnitus is decontextualized. The left lateralization could be related to the left lateralization of the self-referential default mode network (Nielsen et al. 2013), of which the parahippocampus and hippocampus are part (Vincent et al. 2008; Ward et al. 2014). The decontextualized tinnitus sends less information to the subgenual anterior cingulate/ventromedial prefrontal cortex, which is involved in emotional value encoding (Grabenhorst and Rolls 2011; Lipsman et al. 2014; Winecoff et al. 2013), and disrupts priority processing, as emotions drive priority processing (Dolan

Table 5 Correlation of connectivity strength of connections between hubs of tinnitus network that showed a significant difference in connectivity strength after Bonferroni correction in alpha1 frequency band and TQ score controlling for VAS for loudness

Connections	r	p value
Left ITG to Right sgACC	-0.08	0.201
Right PCC1 to Left A1	-0.07	0.253
Right PCC1 to Left ITG	-0.06	0.308
Left ITG to Left A1	-0.04	0.523
Left ITG to Left A2	-0.04	0.550
Left ITG to Left STG	-0.03	0.584

Table 6 Correlation of connectivity strength of connections between hubs of tinnitus network that showed a significant difference in connectivity strength before Bonferroni correction in alpha2 frequency band and TQ score controlling for VAS for loudness

Connections	r	p value
Left HIP2 to Left sgACC	-0.18	0.003
Right IFG to Right TP	-0.17	0.005
Left HIP2 to Right sgACC	-0.16	0.008
Left PHC2 to Right sgACC	-0.14	0.024
Left sgACC to Right TP	-0.12	0.041
Left HIP to Right TP	-0.12	0.042
Left HIP2 to Left MTG	-0.10	0.085
Left dACC to Left Insula	-0.10	0.085
Left Insula to Left MTG	-0.10	0.099
Left HIP2 to Left Insula	-0.10	0.104
Left PHC2 to Left MTG	-0.10	0.107
Left PHC2 to Left Insula	-0.09	0.118
Right VLPFC to Right sgACC	-0.09	0.141
Left ITG to Right sgACC	-0.09	0.151
Left sgACC to Left Insula	-0.09	0.153
Left SMA to Left S1	-0.08	0.158
Right VLPFC to Right TP	-0.08	0.173
Right IFG to Right sgACC	-0.08	0.174
Left A2 to Left PHC2	-0.08	0.188
Left A2 to Left HIP2	-0.07	0.224
Left ITG to Left HIP	-0.07	0.232
Right TP to Right sgACC	-0.07	0.240
Left HIP to Left Insula	-0.07	0.253
Left HIP2 to Left A2	-0.07	0.269
Left HIP2 to Left STG	-0.06	0.281
Left MTG to Left HIP	-0.06	0.294
Left HIP to Left A2	-0.06	0.327
Left dACC to Left SMA	-0.05	0.363
Left HIP to Left MTG	-0.05	0.364
Left ITG to Left MTG	-0.05	0.368
Left HIP to Left STG	-0.05	0.374
Left STG to Left HIP2	-0.05	0.377
Right PreSMA to Left dACC	0.05	0.379
Right sgACC to Left Insula	-0.05	0.381
Left A2 to Left S1	-0.05	0.396
Left PHC2 to Left A2	-0.05	0.419
Left STG to Left S1	-0.05	0.419
Left PHC2 to Left STG	-0.04	0.462
Left ITG to Left A2	-0.04	0.467
Left MTG to Left S1	-0.04	0.481
Left ITG to Left Insula	-0.04	0.491
Left MTG to Left Insula	-0.04	0.491
Left Insula to Left STG	-0.04	0.502
Left HIP to Left ITG	-0.04	0.510
Left Insula to Left A2	-0.04	0.511
Right TP to Left HIP2	0.03	0.565

Table 6 (continued)

Connections	r	p value
Left sgACC to Left MTG	-0.03	0.567
Left MTG to Left PHC2	-0.03	0.577
Right VLPFC to Left HIP	-0.03	0.594
Left sgACC to Left HIP2	-0.03	0.605
Left ITG to Left STG	-0.03	0.605
Left HIP to Left PHC2	-0.03	0.620
Right TP to Left PHC2	0.03	0.629
Left MTG to Left HIP2	-0.03	0.638
Left dACC to Left S1	-0.02	0.687
Left sgACC to Left ITG	-0.02	0.698
Left Insula to left S1	-0.02	0.701
Left sgACC to Left PHC2	-0.02	0.718
Right sgACC to Left HIP2	-0.02	0.771
Right VLPFC to Left HIP2	0.02	0.794
Left MTG to Left STG	0.01	0.813
Right sgACC to Left PHC2	-0.01	0.855
Right sgACC to Left ITG	-0.01	0.892
Left MTG to Left A2	0.01	0.919
Right TP to Left HIP	0.01	0.985

Significant correlations in bold after correction for multiple comparisons using Benjamini Hoshburg False Discovery rate of 25%

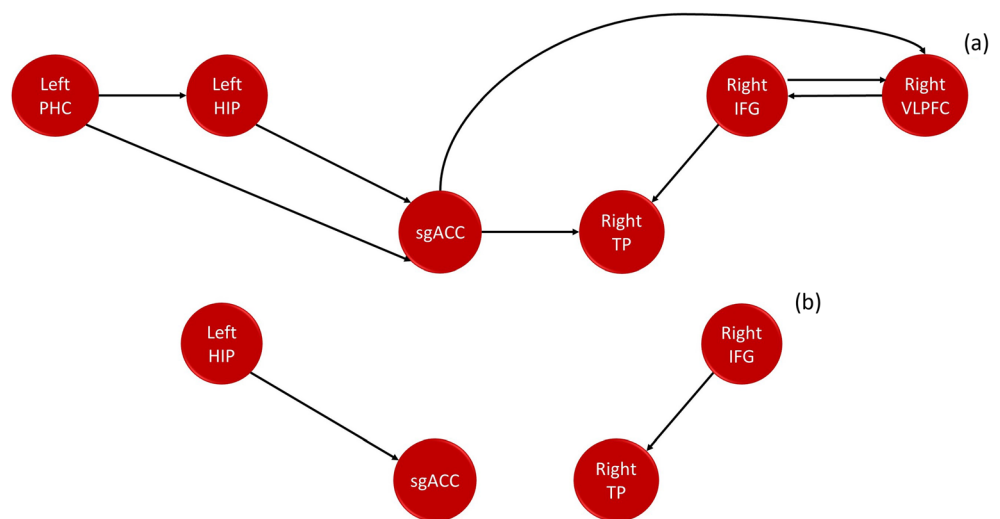
2002). The right ventrolateral prefrontal cortex is part of the emotional ventral attention network (Corbetta et al. 2008; Corbetta and Shulman 2002; Nielsen et al. 2013), and the dorsal temporal pole is also involved in auditory emotional processing (Fan et al. 2014). Thus, in summary, the parahippocampal contextual memory has little influence on the (paradoxical) value that is attached to the phantom sound, which in return has little influence on the emotional attentional processing of the phantom

sound. This suggests that distress is the consequence of the absence of modulation of the phantom sound, or in neurological terms distress is the consequence of the fact that tinnitus cannot be influenced.

Thus, consistent with our hypothesis, we observe that a decrease in connectivity strength between the fronto-limbic regions that characterizes a strong emotional component in tinnitus. These findings agree with the results of other disorders such as schizophrenia, bipolar disorder, major depressive disorder displaying a disconnection of the fronto-limbic circuits (Du et al. 2017; Hong et al. 2015; Mayberg 1997; Radaelli et al. 2015). The relationship of this disconnection with the emotional component was suggested to be due a disintegration of emotional and decision-making regions in two ways (a) due to lack of information going from the limbic regions to the frontal regions or (b) a dysregulation of limbic activity by the frontal regions (Mayberg 1997). In the current study, we observe that tinnitus-related distress is encoded by the former.

However, as opposed to our hypothesis and results of previous functional connectivity studies, we observe a disconnection rather than a hyperconnection between the regions of the medial temporal lobe. It is important to keep in mind that although undirected and directed connectivity seem to be closely related, the former involves only phase information and the latter involves both amplitude and phase information (Blinowska et al. 2004; Pascual-Marqui 2007; Pascual-Marqui et al. 2014). Thus, the deviation from the results of previous functional connectivity studies may be attributed to this fundamental difference between the two techniques. Along with a decrease in connectivity strength, we also observe a decrease in efficiency of information transfer specifically from the hippocampus to the subgenual anterior cingulate cortex forming the crucial location of disconnection between the limbic/temporal lobe regions and the frontal

Fig. 7 Schematic of the core tinnitus distress network obtained from the correlations summarizing the results of the correlations. **a** Core tinnitus distress network obtained from the core tinnitus network whose connections are significantly different from the core control network before Bonferroni correction. **b** Core tinnitus distress network obtained from the core tinnitus network whose connections are significantly different from the core control network after Bonferroni correction



regions. This is confirmed from the significant correlation of the connectivity strength of the hippocampus to the subgenual anterior cingulate cortex with tinnitus-related distress, which is one of the connections that survives multiple comparison when its connectivity strength and path length was compared to that of the control group.

The results of the current study contribute an important piece in the distress literature since it not only identifies the core distress network but also provides directional information which may be used to identify more efficient targets for future neuromodulatory studies. For example, from the conclusions from our previous study, a network may be most rapidly modulated by modulating not the hubs of the core network, but a node that directly connects to the hub of the core network, i.e. a connector hub (Mohan et al. 2016c). From the results of a previous neuromodulatory study targeting the dorsal anterior cingulate cortex to reduce distress, authors observed that responders have higher functional connectivity between the parahippocampus and subgenual anterior cingulate cortex in the alpha frequency band (De Ridder et al. 2015b), the main disconnecting link identified in the current study. The dorsal anterior cingulate cortex, although not present in the core distress network connects to the hubs of the core distress network. Thus, it would be interesting to see if targeting this specific link by modulating the dorsal anterior cingulate cortex would result in strengthening the connection from the parahippocampus to the subgenual anterior cingulate cortex, thus improving tinnitus distress better than previous studies did.

Further, several studies in the past show that distress is a disorder-general symptom that accompanies several pathologies apart from tinnitus and is also encoded by a common distress network. Thus, the core distress network identified in tinnitus could be extended to other pathologies as well. Thus, the disconnection between the parahippocampus and the subgenual anterior cingulate may serve as a neuromodulatory target not just for tinnitus but other pathologies as well. Finally, the current study only looks at the core distress network and not the complete network which is a critical piece in understanding the complete dynamics of the distress network. Thus, the results of the current study may serve as a foundation for future research identifying the neural correlates of distress.

Limitations

The current study identifies the core tinnitus distress network but with some limitations. Several studies in the field present an important relationship between hearing loss and tinnitus. Thus, the first limitation of the current study is that the control group is not matched for hearing loss. However, hearing loss is more associated with the loudness component than the emotional component of tinnitus, which is the focus of the current study. Nevertheless, future studies replicating the current

study with a control group matched for hearing loss will be able to bolster the results of the current study. Secondly, tinnitus distress has been shown to involve deeper subcortical structures are more reliably localized using other imaging techniques. However, this is the first study that we know of that uses effective connectivity to determine the core tinnitus distress network in a data-driven way. Thus, the current study lays a foundation for future studies that could use fMRI or other spatially strong techniques to tell us how deeper subcortical structure may affect the dynamics of the network discussed in the current study.

Conclusion

The current study shows that directed functional networks underlying tinnitus show a disconnection mainly between the frontal, temporal, medial temporal and cingulate regions, some of which form the important hubs of the tinnitus network in the alpha frequency bands. The disconnection is characterized by decreased connectivity strength and efficiency of information transfer, with the tinnitus network shifting from a small-world to a less efficient lattice topology. The distinct hubs of the core tinnitus network also show decreased connectivity and efficiency of information transfer amongst themselves, suggesting decreased functional integration between modules. The core distress network consists of the hubs of the default mode network (parahippocampus) and the emotional processing centers (subgenual anterior cingulate/ventromedial prefrontal cortex). Such a disconnection suggests that the parahippocampal contextual memory has little influence on the (paradoxical) value that is attached to the phantom sound and that distress is the consequence of the absence of modulation of the phantom sound.

Compliance with ethical standards

Conflict of interest The authors declare no competing financial or conflict of other interests.

Research involving human participants This study was approved by the local ethical committee (Antwerp University Hospital) and was in accordance with the declaration of Helsinki. Collection of the data was done under the approval of IRB UZA OGA85. All patients gave their written informed consent.

Publisher's Note Springer Nature remains neutral with regard to jurisdictional claims in published maps and institutional affiliations.

References

- Aminoff, E., Gronau, N., & Bar, M. (2007). The parahippocampal cortex mediates spatial and nonspatial associations. *Cerebral Cortex*, 17(7), 1493–1503. <https://doi.org/10.1093/cercor/bhl078>.

- Aminoff, E. M., Kveraga, K., & Bar, M. (2013). The role of the parahippocampal cortex in cognition. *Trends in Cognitive Sciences*, 17(8), 379–390. <https://doi.org/10.1016/j.tics.2013.06.009>.
- Axelsson, A., & Ringdahl, A. (1989). Tinnitus—a study of its prevalence and characteristics. *British Journal of Audiology*, 23(1), 53–62.
- Bassett, D. S., Bullmore, E., Verchinski, B. A., Mattay, V. S., Weinberger, D. R., & Meyer-Lindenberg, A. (2008). Hierarchical organization of human cortical networks in health and schizophrenia. *The Journal of Neuroscience*, 28(37), 9239–9248. <https://doi.org/10.1523/JNEUROSCI.1929-08.2008>.
- Benjamini, Y., & Hochberg, Y. (1995). Controlling the false discovery rate: a practical and powerful approach to multiple testing. *Journal of the Royal Statistical Society: Series B (Methodological)*, 57(1), 289–300.
- Blinowska, K. J., Kuś, R., & Kamiński, M. (2004). Granger causality and information flow in multivariate processes. *Physical Review E*, 70(5), 050902.
- Bullmore, E., & Sporns, O. (2009). Complex brain networks: graph theoretical analysis of structural and functional systems. *Nature Reviews. Neuroscience*, 10(3), 186–198.
- Bullmore, E., & Sporns, O. (2012). The economy of brain network organization. *Nature Reviews. Neuroscience*, 13(5), 336–349. <https://doi.org/10.1038/nrn3214>.
- Chen, Y.-C., Bo, F., Xia, W., Liu, S., Wang, P., Su, W., ... Yin, X. (2017a). Amygdala functional disconnection with the prefrontal-cingulate-temporal circuit in chronic tinnitus patients with depressive mood. *Progress in Neuro-Psychopharmacology and Biological Psychiatry*, 79, 249–257. <https://doi.org/10.1016/j.pnpbp.2017.07.001>.
- Chen, Y. C., Xia, W., Chen, H., Feng, Y., Xu, J. J., Gu, J. P., ... Yin, X. (2017b). Tinnitus distress is linked to enhanced resting-state functional connectivity from the limbic system to the auditory cortex. *Human Brain Mapping*, 38, 2384–2397.
- Corbetta, M., & Shulman, G. L. (2002). Control of goal-directed and stimulus-driven attention in the brain. *Nature Reviews. Neuroscience*, 3(3), 201–215. <https://doi.org/10.1038/nrn755>.
- Corbetta, M., Patel, G., & Shulman, G. L. (2008). The reorienting system of the human brain: from environment to theory of mind. *Neuron*, 58(3), 306–324. <https://doi.org/10.1016/j.neuron.2008.04.017>.
- Crossley, N. A., Mechelli, A., Scott, J., Carletti, F., Fox, P. T., McGuire, P., & Bullmore, E. T. (2014). The hubs of the human connectome are generally implicated in the anatomy of brain disorders. *Brain*, 137(8), 2382–2395. <https://doi.org/10.1093/brain/awu132>.
- de Haan, W., Pijnenburg, Y. A. L., Strijers, R. L. M., van der Made, Y., van der Flier, W. M., Scheltens, P., & Stam, C. J. (2009). Functional neural network analysis in frontotemporal dementia and Alzheimer's disease using EEG and graph theory. *BMC Neuroscience*, 10, 101–101. <https://doi.org/10.1186/1471-2202-10-101>.
- De Ridder, D., & Vanneste, S. (2014). Targeting the Parahippocampal area by auditory cortex stimulation in tinnitus. *Brain Stimulation*, 7, 709–717. <https://doi.org/10.1016/j.brs.2014.04.004>.
- De Ridder, D., Franssen, H., Francois, J., Sunaert, S., Kovacs, S., & Van De Heyning, P. (2006). Amygdalohippocampal involvement in tinnitus and auditory memory. *Acta Oto-Laryngologica. Supplementum*, 126(556), 50–53.
- De Ridder, D., Elgoyhen, A. B., Romo, R., & Langguth, B. (2011a). Phantom percepts: tinnitus and pain as persisting aversive memory networks. *Proceedings of the National Academy of Sciences of the United States of America*, 108(20), 8075–8080. <https://doi.org/10.1073/pnas.1018466108>.
- De Ridder, D., Vanneste, S., & Congedo, M. (2011b). The distressed brain: a group blind source separation analysis on tinnitus. *PLoS One*, 6(10), e24273. <https://doi.org/10.1371/journal.pone.0024273>.
- De Ridder, D., Vanneste, S., Weisz, N., Londero, A., Schlee, W., Elgoyhen, A. B., & Langguth, B. (2014a). An integrative model of auditory phantom perception: tinnitus as a unified percept of interacting separable subnetworks. *Neuroscience and Biobehavioral Reviews*, 44, 16–32. <https://doi.org/10.1016/j.neubiorev.2013.03.021>.
- De Ridder, D., Vanneste, S., & Freeman, W. (2014b). The Bayesian brain: phantom percepts resolve sensory uncertainty. *Neuroscience and Biobehavioral Reviews*, 44, 4–15. <https://doi.org/10.1016/j.neubiorev.2012.04.001>.
- De Ridder, D., Congedo, M., & Vanneste, S. (2015a). The neural correlates of subjectively perceived and passively matched loudness perception in auditory phantom perception. *Brain and Behavior*, 5(5), e00331. <https://doi.org/10.1002/brb3.331>.
- De Ridder, D., Joos, K., & Vanneste, S. (2015b). Anterior cingulate implants for tinnitus: report of 2 cases. *Journal of Neurosurgery*, 124(4), 893–901. <https://doi.org/10.3171/2015.3.JNS142880>.
- De Ridder, D., Vanneste, S., Langguth, B., & Llinas, R. (2015c). Thalamocortical dysrhythmia: a theoretical update in tinnitus. *Frontiers in Neurology*, 6, 124. <https://doi.org/10.3389/fneur.2015.00124>.
- Dijkstra, E. W. (1959). A note on two problems in connexion with graphs. *Numerische Mathematik*, 1(1), 269–271. <https://doi.org/10.1007/BF01386390>.
- Dolan, R. J. (2002). Emotion, cognition, and behavior. *Science*, 298(5596), 1191–1194. <https://doi.org/10.1126/science.1076358>.
- Du, L., Zeng, J., Liu, H., Tang, D., Meng, H., Li, Y., & Fu, Y. (2017). Fronto-limbic disconnection in depressed patients with suicidal ideation: a resting-state functional connectivity study. *Journal of Affective Disorders*, 215, 213–217.
- Elgoyhen, A. B., Langguth, B., De Ridder, D., & Vanneste, S. (2015). Tinnitus: perspectives from human neuroimaging. *Nature Reviews Neuroscience*, 16(10), 632–642.
- Fan, L., Wang, J., Zhang, Y., Han, W., Yu, C., & Jiang, T. (2014). Connectivity-based parcellation of the human temporal pole using diffusion tensor imaging. *Cerebral Cortex*, 24(12), 3365–3378. <https://doi.org/10.1093/cercor/bht196>.
- Fornito, A., & Bullmore, E. T. (2014). Connectomics: a new paradigm for understanding brain disease. *European Neuropsychopharmacology*, 25, 733–748. <https://doi.org/10.1016/j.euroneuro.2014.02.011>.
- Fornito, A., & Bullmore, E. T. (2015). Reconciling abnormalities of brain network structure and function in schizophrenia. *Current Opinion in Neurobiology*, 30, 44–50. <https://doi.org/10.1016/j.conb.2014.08.006>.
- Fornito, A., Zalesky, A., & Breakspear, M. (2015). The connectomics of brain disorders. *Nature Reviews. Neuroscience*, 16(3), 159–172. <https://doi.org/10.1038/nrn3901>.
- Friston, K. J. (2011). Functional and effective connectivity: a review. *Brain Connectivity*, 1(1), 13–36.
- Friston, K. J., & Frith, C. D. (1995). Schizophrenia: a disconnection syndrome. *Clinical Neuroscience*, 3(2), 89–97.
- Friston, K., Brown, H. R., Siemerker, J., & Stephan, K. E. (2016). The dysconnection hypothesis. *Schizophrenia Research*. <https://doi.org/10.1016/j.schres.2016.07.014>.
- Görtelmeyer, R., Schmidt, J., Suckfüll, M., Jastreboff, P., Gebauer, A., Krüger, H., & Wittmann, W. (2011). Assessment of tinnitus-related impairments and disabilities using the German THI-12: sensitivity and stability of the scale over time. *International Journal of Audiology*, 50, 523–529. <https://doi.org/10.3109/14992027.2011.578591>.
- Grabenhorst, F., & Rolls, E. T. (2011). Value, pleasure and choice in the ventral prefrontal cortex. *Trends in Cognitive Sciences*, 15(2), 56–67. <https://doi.org/10.1016/j.tics.2010.12.004>.
- Hong, S. B., Harrison, B. J., Fornito, A., Sohn, C. H., Song, I. C., & Kim, J. W. (2015). Functional dysconnectivity of corticostriatal circuitry and differential response to methylphenidate in youth with attention-deficit/hyperactivity disorder. *Journal of Psychiatry & Neuroscience*, 40(1), 46–57.
- Hu, X., Song, X., Yuan, Y., Li, E., Liu, J., Liu, W., & Liu, Y. (2015). Abnormal functional connectivity of the amygdala is associated

- with depression in Parkinson's disease. *Movement Disorders*, 30(2), 238–244. <https://doi.org/10.1002/mds.26087>.
- Jastreboff, P. J. (1990). Phantom auditory perception (tinnitus): mechanisms of generation and perception. *Neuroscience Research*, 8(4), 221–254.
- Klimesch, W. (2012). Alpha-band oscillations, attention, and controlled access to stored information. *Trends in Cognitive Sciences*, 16(12), 606–617. <https://doi.org/10.1016/j.tics.2012.10.007>.
- Klimesch, W., Sauseng, P., & Hanslmayr, S. (2007). EEG alpha oscillations: the inhibition–timing hypothesis. *Brain Research Reviews*, 53(1), 63–88. <https://doi.org/10.1016/j.brainresrev.2006.06.003>.
- Krishnadas, R., Ryali, S., Chen, T., Uddin, L., Supekar, K., Palaniyappan, L., & Menon, V. (2014). Resting state functional hyperconnectivity within a triple network model in paranoid schizophrenia. *The Lancet*, 383, S65. [https://doi.org/10.1016/S0140-6736\(14\)60328-7](https://doi.org/10.1016/S0140-6736(14)60328-7).
- Lancaster, J. L., Woldorff, M. G., Parsons, L., Liotti, M., Freitas, C., Rainey, L., ... Fox, P. (2000). Automated Talairach atlas labels for functional brain mapping. *Human Brain Mapping*, 10(3), 120–131.
- Laureano, M. R., Onishi, E. T., Bressan, R. A., Castiglioni, M. L., Batista, I. R., Reis, M. A., ... Jackowski, A. P. (2014). Memory networks in tinnitus: a functional brain image study. *PLoS One*, 9(2), e87839. <https://doi.org/10.1371/journal.pone.0087839>.
- Lipsman, N., Kaping, D., Westendorff, S., Sankar, T., Lozano, A. M., & Womelsdorf, T. (2014). Beta coherence within human ventromedial prefrontal cortex precedes affective value choices. *Neuroimage*, 85(Pt 2), 769–778. <https://doi.org/10.1016/j.neuroimage.2013.05.104>.
- Llinás, R. R., Ribary, U., Jeanmonod, D., Kronberg, E., & Mitra, P. P. (1999). Thalamocortical dysrhythmia: a neurological and neuropsychiatric syndrome characterized by magnetoencephalography. *Proceedings of the National Academy of Sciences*, 96(26), 15222–15227.
- Mayberg, H. S. (1997). Limbic-cortical dysregulation: a proposed model of depression. *The Journal of Neuropsychiatry and Clinical Neurosciences*, 9(3), 471–481.
- Meeus, O., Blavie, C., & Van de Heyning, P. (2007). Validation of the Dutch and the French version of the tinnitus questionnaire. *B-ENT*, 3(Suppl 7), 11–17.
- Meeus, O., Heyndrickx, K., Lambrechts, P., De Ridder, D., & Van de Heyning, P. (2010). Phase-shift treatment for tinnitus of cochlear origin. *European Archives of Oto-Rhino-Laryngology*, 267(6), 881–888. <https://doi.org/10.1007/s00405-009-1145-y>.
- Meeus, O., De Ridder, D., & Van de Heyning, P. (2011). Administration of the Combination Clonazepam-Deanxit as treatment for tinnitus. *Otology & Neurotology*, 32(4), 701–709. <https://doi.org/10.1097/MAO.0b013e31820e737c>.
- Mohan, A., & Vanneste, S. (2017). Adaptive and maladaptive neural compensatory consequences of sensory deprivation – From a phantom percept perspective. *Progress in Neurobiology*, 1531–17. <https://doi.org/10.1016/j.pneurobio.2017.03.010>
- Mohan, A., De Ridder, D., & Vanneste, S. (2016a). Emerging hubs in phantom perception connectomics. *NeuroImage: Clinical*, 11, 181–194. <https://doi.org/10.1016/j.nicl.2016.01.022>.
- Mohan, A., De Ridder, D., & Vanneste, S. (2016b). Graph theoretical analysis of brain connectivity in phantom sound perception. *Scientific Reports*, 6, 19683. <https://doi.org/10.1038/srep19683>.
- Mohan, A., De Ridder, D., & Vanneste, S. (2016c). Robustness and dynamicity of functional networks in phantom sound. *NeuroImage*. <https://doi.org/10.1016/j.neuroimage.2016.04.033>.
- Nielsen, J. A., Zielinski, B. A., Ferguson, M. A., Lainhart, J. E., & Anderson, J. S. (2013). An evaluation of the left-brain vs. right-brain hypothesis with resting state functional connectivity magnetic resonance imaging. *PLoS One*, 8(8), e71275. <https://doi.org/10.1371/journal.pone.0071275>.
- Olde Dubbelink, K. T. E., Hillebrand, A., Stoffers, D., Deijen, J. B., Twisk, J. W. R., Stam, C. J., & Berendse, H. W. (2014). Disrupted brain network topology in Parkinson's disease: a longitudinal magnetoencephalography study. *Brain*, 137(1), 197–207. <https://doi.org/10.1093/brain/awt316>
- Pascual-Marqui, R. D. (2002). Standardized low resolution brain electromagnetic tomography (sLORETA): technical details. *Methods and Findings in Experimental and Clinical Pharmacology*, 24(Suppl D), 5–12.
- Pascual-Marqui, R. D. (2007). Instantaneous and lagged measurements of linear and nonlinear dependence between groups of multivariate time series: frequency decomposition. *arXiv preprint arXiv:0711.1455*. <https://arxiv.org/abs/0711.1455>. Accessed Sept 1, 2018
- Assessing direct paths of intracortical causal information flow of oscillatory activity with the isolated effective coherence (iCoh). *Frontiers in human neuroscience*, 8. <https://doi.org/10.3389/fnhum.2014.00448>.
- Radaelli, D., Papa, G. S., Vai, B., Poletti, S., Smeraldi, E., Colombo, C., & Benedetti, F. (2015). Fronto-limbic disconnection in bipolar disorder. *European Psychiatry*, 30(1), 82–88.
- Rubinov, M., & Sporns, O. (2010). Complex network measures of brain connectivity: uses and interpretations. *NeuroImage*, 52(3), 1059–1069. <https://doi.org/10.1016/j.neuroimage.2009.10.003>.
- Sanz-Arigita, E. J., Schoonheim, M. M., Damoiseaux, J. S., Rombouts, S. A., Maris, E., Barkhof, F., ... Stam, C. J. (2010). Loss of 'small-world' networks in Alzheimer's disease: graph analysis of FMRI resting-state functional connectivity. *PLoS One*, 5(11), e13788. <https://doi.org/10.1371/journal.pone.0013788>.
- Song, J. J., De Ridder, D., Van de Heyning, P., & Vanneste, S. (2012). Mapping tinnitus-related brain activation: an activation-likelihood estimation metaanalysis of PET studies. *Journal of Nuclear Medicine*. <https://doi.org/10.2967/jnumed.112.102939>.
- Sporns, O. (2013). Network attributes for segregation and integration in the human brain. *Current Opinion in Neurobiology*, 23(2), 162–171. <https://doi.org/10.1016/j.conb.2012.11.015>.
- Sripada, R. K., King, A. P., Garfinkel, S. N., Wang, X., Sripada, C. S., Welsh, R. C., & Liberzon, I. (2012). Altered resting-state amygdala functional connectivity in men with posttraumatic stress disorder. *Journal of Psychiatry & Neuroscience: JPN*, 37(4), 241–249. <https://doi.org/10.1503/jpn.110069>.
- Stam, C. J. (2014). Modern network science of neurological disorders. *Nature Reviews. Neuroscience*, 15(10), 683–695. <https://doi.org/10.1038/nrn3801>.
- Stephan, K. E., Friston, K. J., & Frith, C. D. (2009). Dysconnection in schizophrenia: from abnormal synaptic plasticity to failures of self-monitoring. *Schizophrenia Bulletin*, 35(3), 509–527. <https://doi.org/10.1093/schbul/sbn176>.
- Toth, M., Kiss, A., Kosztlanyi, P., & Kondakor, I. (2007). Diurnal alterations of brain electrical activity in healthy adults: a LORETA study. *Brain Topography*, 20(2), 63–76. <https://doi.org/10.1007/s10548-007-0032-3>.
- Uhlhaas, P. J. (2013). Dysconnectivity, large-scale networks and neuronal dynamics in schizophrenia. *Current Opinion in Neurobiology*, 23(2), 283–290. <https://doi.org/10.1016/j.conb.2012.11.004>.
- Vanneste, S., Focquaert, F., Van de Heyning, P., & De Ridder, D. (2011a). Different resting state brain activity and functional connectivity in patients who respond and not respond to bifrontal tDCS for tinnitus suppression. *Experimental Brain Research*, 210(2), 217–227. <https://doi.org/10.1007/s00221-011-2617-z>.
- Vanneste, S., van de Heyning, P., & De Ridder, D. (2011b). The neural network of phantom sound changes over time: a comparison between recent-onset and chronic tinnitus patients. *European Journal of Neuroscience*, 34(5), 718–731. <https://doi.org/10.1111/j.1460-9568.2011.07793.x>.
- Vanneste, S., Congedo, M., & De Ridder, D. (2014). Pinpointing a highly specific pathological functional connection that turns phantom sound into distress. *Cerebral Cortex*, 24(9), 2268–2282.

- Vanneste, S., Faber, M., Langguth, B., & De Ridder, D. (2016). The neural correlates of cognitive dysfunction in phantom sounds. *Brain Research, 1642*, 170–179. <https://doi.org/10.1016/j.brainres.2016.03.016>.
- Vincent, J. L., Kahn, I., Snyder, A. Z., Raichle, M. E., & Buckner, R. L. (2008). Evidence for a frontoparietal control system revealed by intrinsic functional connectivity. *Journal of Neurophysiology, 100*(6), 3328–3342. <https://doi.org/10.1152/jn.90355.2008>.
- von Leupoldt, A., Sommer, T., Kegat, S., Baumann, H. J., Klose, H., Dahme, B., & Büchel, C. (2009). Dyspnea and pain share emotion-related brain network. *NeuroImage, 48*(1), 200–206.
- Ward, A. M., Schultz, A. P., Huijbers, W., Van Dijk, K. R., Hedden, T., & Sperling, R. A. (2014). The parahippocampal gyrus links the default-mode cortical network with the medial temporal lobe memory system. *Human Brain Mapping, 35*(3), 1061–1073. <https://doi.org/10.1002/hbm.22234>.
- Watts, D. J. (1999). Networks, dynamics, and the small-world phenomenon. *American Journal of Sociology, 105*(2), 493–527. <https://doi.org/10.1086/210318>.
- Watts, D. J., & Strogatz, S. H. (1998). Collective dynamics of 'small-world' networks. *Nature, 393*(6684), 440–442. <https://doi.org/10.1038/30918>.
- Weinberger, D. R. (1993). A connectionist approach to the prefrontal cortex. *The Journal of Neuropsychiatry and Clinical Neurosciences, 5*(3), 241–53.
- Williams, L. M., Das, P., Liddell, B. J., Olivieri, G., Peduto, A. S., David, A. S., . . . Harris, A. W. F. (2007). Fronto-limbic and autonomic disjunctions to negative emotion distinguish schizophrenia subtypes. *Psychiatry Research: Neuroimaging, 155*(1), 29–44. <https://doi.org/10.1016/j.psychres.2006.12.018>.
- Winecoff, A., Clithero, J. A., Carter, R. M., Bergman, S. R., Wang, L., & Huettel, S. A. (2013). Ventromedial prefrontal cortex encodes emotional value. *The Journal of Neuroscience, 33*(27), 11032–11039. <https://doi.org/10.1523/JNEUROSCI.4317-12.2013>.
- Zeman, F., Koller, M., Schecklmann, M., Langguth, B., & Landgrebe, M. (2012). Tinnitus assessment by means of standardized self-report questionnaires: psychometric properties of the tinnitus questionnaire (TQ), the tinnitus handicap inventory (THI), and their short versions in an international and multi-lingual sample. *Health and Quality of Life Outcomes, 10*(1), 1–10. <https://doi.org/10.1186/1477-7525-10-128>.
- Zhang, J., Cheng, W., Liu, Z., Zhang, K., Lei, X., Yao, Y., . . . Lu, G. (2016). Neural, electrophysiological and anatomical basis of brain-network variability and its characteristic changes in mental disorders. *Brain, 139*(8), 2307–2321.